Journal of Medicinal Chemistry

Article

pubs.acs.org/jmc

A New Strategy for the Development of Highly Potent and Selective Plasmin Inhibitors

Sebastian M. Saupe and Torsten Steinmetzer*

Department of Pharmacy, Institute of Pharmaceutical Chemistry, Philipps University Marburg, Marbacher Weg 6, D-35032 Marburg, Germany

Supporting Information

ABSTRACT: A new structure-based strategy for the design of potent and selective plasmin inhibitors was developed. These compounds could be prepared by cyclizations between the P3 and P2 amino acid residues of substrate-analogue inhibitors using metathesis or a copper-catalyzed azide alkyne cycloaddition in combination with standard peptide couplings. The most potent bis-triazole derivative **10** inhibits plasmin and plasma kallikrein with K_i of 0.77 and 2.4 nM, respectively, whereas it has poor activity against the related trypsin-like serine proteases thrombin, factor Xa, or activated protein C. Modeling experiments revealed that inhibitor **10** adopts a compact and rigid structure that fits well into the relatively open active site of plasmin and plasma kallikrein, while it is rejected from sterically demanding residues present in loops of the other enzymes. These results from modeling confirm the selectivity profile found for inhibitor **10** in enzyme kinetic studies. Such compounds might be useful lead structures for the development of new antifibrinolytic drugs for use in cardiac surgery with cardiopulmonary bypass or organ transplantations to reduce bleeding complications.

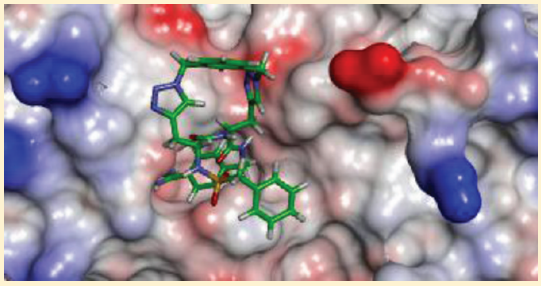

INTRODUCTION

The family of trypsin-like serine proteases contains more than 70 members, which are involved in many physiological and pathological processes. Although all of them cleave their substrates after the basic amino acids arginine or lysine, there are big differences in their substrate specificities. Some of them, like the clotting factor Xa, are highly specific and process only very few natural substrates. Others, like the digestive protease trypsin, are relatively unspecific and hydrolyze a variety of different substrates. An additional nonspecific trypsin-like serine protease is the fibrinolytic enzyme plasmin, an antagonist of the clotting proteases, which is responsible for the degradation of fibrin clots in blood. Therefore, plasmin inhibitors can be used for the treatment of hyperfibrinolysis, which may occur during cardiac surgery with cardiopulmonary bypass or organ transplantation. Aprotinin, a 58 amino acid long peptidic plasmin inhibitor isolated from bovine lung, was clinically used to reduce blood loss under these conditions over many years. However, because of later reported side effects,[1] such as an increased number of heart attacks and kidney damage, aprotinin was withdrawn from market in 2008. Presently, only tranexamic acid or *p*-aminomethylbenzoic acid can be used as alternative antifibrinolytics. However, both compounds inhibit only the plasminogen activation but have no direct inhibitory effect on already formed plasmin. Therefore, the development of new effective and selective plasmin inhibitors as replacement for aprotinin is of special therapeutic interest. In contrast to the large number of potent inhibitors developed for the clotting proteases thrombin and factor Xa,[2] only a few synthetic plasmin inhibitors have been described so far. For instance, the Okada group has developed several inhibitors with IC_{50} of approximately 0.5 μM containing a *trans*-4-aminomethylcyclohexanecarboxylic acid residue.[3,4] A series of cyclic ketone-based inhibitors with K_i > 1 μM has been described by Seto.[5,6] Solid phase peptide synthesis was recently used to prepare potent peptidic arginal-derived plasmin inhibitors (see known structures below).[7]

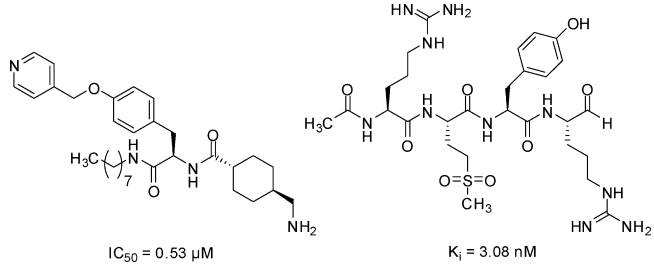

Received: September 9, 2011
Published: January 25, 2012

 © 2012 American Chemical Society

How is it possible to develop selective plasmin inhibitors, although the trypsin-like serine proteases share a significant sequence identity in their protease domains? A closer comparison of their primary structure reveals that in plasmin a loop segment around the amino acid in position 99 is completely missing. The direct connection between the plasmin residue 94 and the amino acid in position 101 is named as 94-shunt and a unique structural feature of plasmin (Figure 1).[8]

In addition, a comparison of the crystal structures available for more than 25 different trypsin-like serine proteases reveals that the size of the amino acid in position 99 has a major influence on possible P2 residues found in substrates and substrate-analogue inhibitors of these enzymes (the terms P1, P2, and P3 of the amino acid positions in substrates and the binding pockets S1, S2, and S3 within the active site of the protease correspond to the nomenclature of Schechter and Berger).[9] For instance, factor Xa containing a sterically demanding tyrosine in position 99 preferentially cleaves substrates with glycine in P2 position,[10] whereas PK possessing a glycine 99 prefers more bulky P2 amino acids, e.g., phenylalanine.[11] This residue 99 also belongs to an active site loop that spatially separates the proximal S2 from the distal S3/S4 binding pocket in trypsin-like serine proteases. Therefore, the missing segment 95−100 leads to a unique open active site in the case of plasmin, due to a fusion of its proximal and distal binding pockets.[2] Most likely, this is the main cause for plasmin being a relatively nonspecific protease that cleaves many different substrates as long as they contain a basic amino acid in P1 position. The structural differences between plasmin and the other trypsin-like serine proteases around their 99-loop are shown in Figure 2.

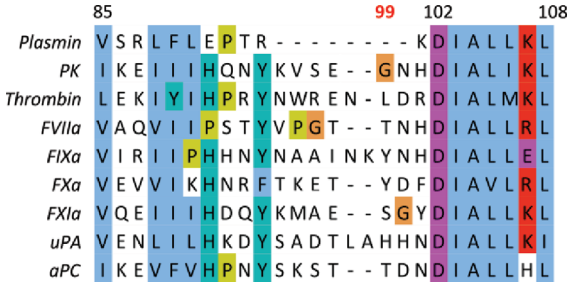

Figure 1. ClustalW multiple sequence alignment of the protease domains from physiologically relevant trypsin-like serine proteases around the amino acid in position 99 (PK, plasma kallikrein; FXa, factor Xa; uPA, urokinase-type plasminogen activator; aPC, activated protein C). The sequence positions are labeled according to the chymotrypsinogen-numbering.

Various groups have developed substrate-analogue inhibitors of trypsin-like serine proteases containing a decarboxylated arginine mimetic as P1 residue, e.g., a 4-amidinobenzylamide. It was often combined with a P2 residue in L-configuration and a D-amino acid in P3 position,[13,14] whereas a benzylsulfonyl moiety was used as the P4 group.[15,16] During the development of inhibitors for the coagulation proteases thrombin and factor Xa the fibrinolytic plasmin was normally an antitarget and should not be inhibited. On the other hand, we have also found among these derivatives several potent plasmin inhibitors, such as compound **1** (Figure 3). However, all of these compounds suffered from relatively poor selectivity; e.g., inhibitor **1** inhibits plasmin, PK, and aPC with inhibition constants of <1 nM (Table 2).[17] Such a low selectivity could be a disadvantage for further drug development because it may lead to more side effects.

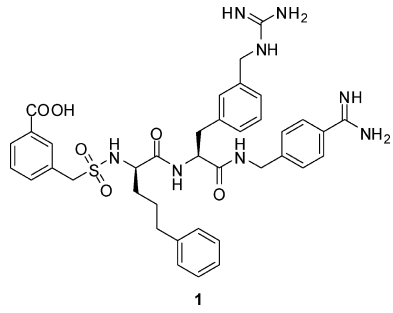

1

Figure 3. Structure of the linear nonspecific inhibitor **1**.

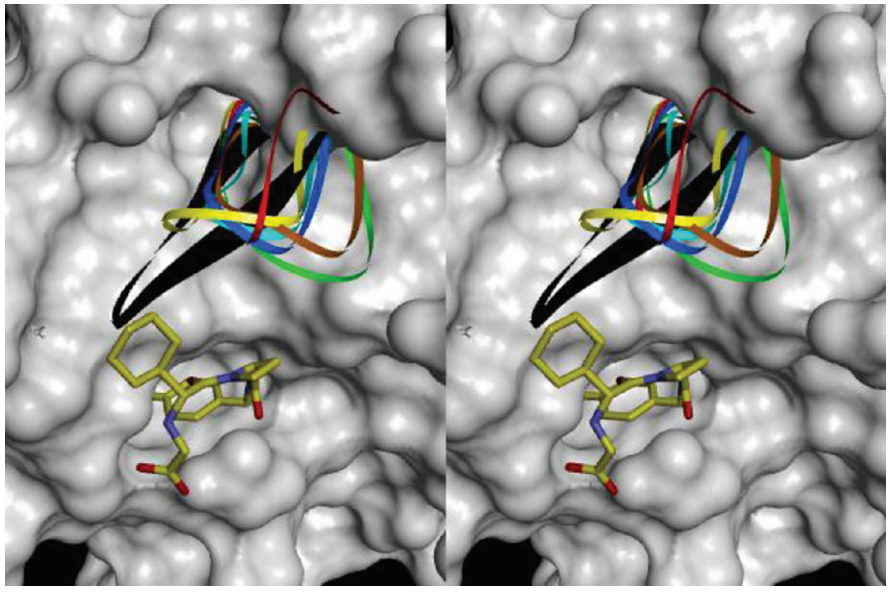

Figure 2. Stereoview of plasmin (1bui.pdb, shown as gray surface) overlaid with the structures of relevant trypsin-like serine proteases. For clarity, only the hairpin loops around their amino acid in position 99 are shown for the other enzymes (FIXa, 3lc3.pdb in red; FVIIa, 1klj, green; FXa, 2pr3, dark blue; PK, 2any, brown; thrombin, 1k22, yellow; uPA, 1vja, black; aPC, 1aut, light blue). These loops protrude from the surface because it is completely missing in plasmin. To clarify the active site, the substrate-analogue thrombin inhibitor melagatran (1k22.pdb) is shown with yellow carbon atoms.[12]

dx.doi.org/10.1021/jm2011996 | J. Med. Chem. 2012, 55, 1171−1180

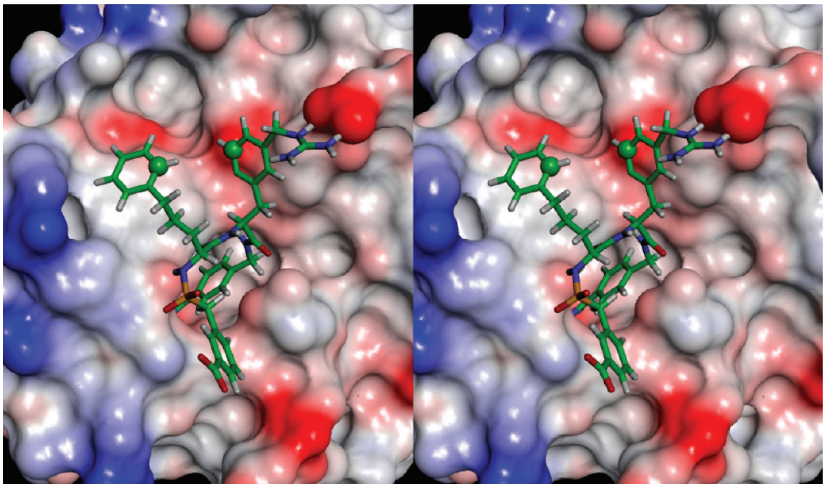

Figure 4. Stereoview of the modeled structure of inhibitor **1** in plasmin. The P2 guanidino group binds to Glu60, whereas the P3 phenyl ring is located above Trp215. Both side chains of the P2 and P3 amino acids are directed toward the enzyme surface and located relatively close to each other. The distance between the two carbon atoms, which are exemplarily shown as green balls, is 4.9 Å.

On the basis of many crystal structures of substrate-analogue inhibitors, which all bind in the form of an antiparallel β-sheet to the trypsin-like serine proteases,[10,15,16,18] it is known that the P2 and P3 side chains point in the same direction toward the enzyme surface, like in melagatran (Figure 2) or in the manually modeled structure of inhibitor **1** in plasmin (Figure 4). Therefore, we have assumed that it might be possible to design potent plasmin inhibitors by appropriate cyclization between these side chains. Such cyclized inhibitors should still be able to bind to the relatively open binding pocket of plasmin. In addition, their rigid cyclic structure should induce a steric repulsion from the 99-loop present in all other trypsin-like serine proteases, which should improve the selectivity of this type of plasmin inhibitor. In this manuscript we communicate our results regarding the synthesis and enzyme kinetic characterization of these new cyclic plasmin inhibitors.

RESULTS

Synthesis. In analogy to the acyclic reference compound **1** the 4-amidinobenzylamide anchor in the P1 position was retained. In contrast, a nonsubstituted benzylsulfonyl group was used as P4 residue for two reasons. On the basis of the model shown in Figure 4, the carboxyl group is directed into the solvent and not involved in specific contacts to plasmin. Second, it is known from previous selectivity studies with structurally related substrate-analogue urokinase[18] and factor Xa[19] inhibitors that a 3-COOH-benzylsulfonyl residue in P4 position leads to a 3- to 5-fold reduced plasmin affinity compared to analogues without carboxyl substitution. To simplify the synthesis, we generally incorporated amino acids with identical side chain functionalities in P2 and P3 positions, which allowed a nondirectional cyclization with symmetrical bridging groups.

Three different strategies were used for the cyclization. First, inhibitors **2**–**7** were prepared by connecting the P2 and P3 side chains via an appropriate linker moiety by amide bond formation, as exemplarily shown for inhibitor **6** in Scheme 1. The D- and L-3-aminomethylphenylalanine derivatives required for the synthesis of intermediate **13** and its para-analogues required for the preparation of inhibitors **3** and **4** were obtained by hydrogenation of N-terminal protected cyanophenylalanines (see Supporting Information).

Scheme 1. Synthesis of Inhibitor 6[a]

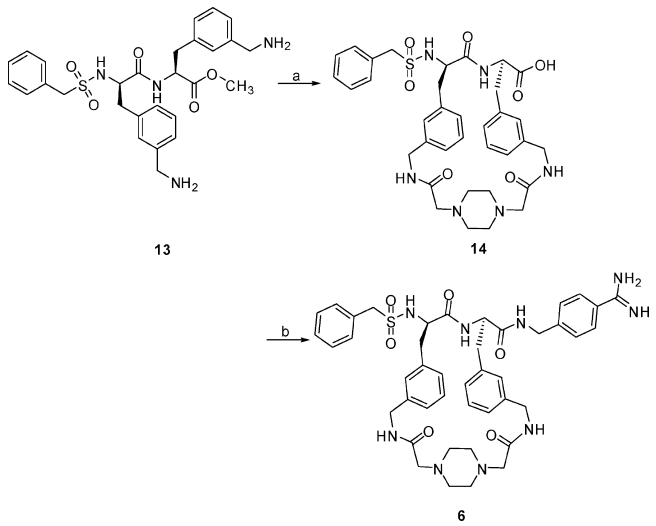

[a](a) (i) 1 equiv of *N*,*N*′-1,4-piperazinediacetic acid, 2 equiv of PyBOP, 6 equiv of DIPEA, DMF, 0 °C; (ii) 3.2 equiv of 1 N NaOH, ethanol/water, room temp, preparative HPLC, 37% yield (two steps); (b) 1 equiv of 4-Amba·2 HCl, 1 equiv of PyBOP, 4 equiv of DIPEA, DMF, 0 °C, preparative HPLC, 63% yield.

Meanwhile, metathesis is a well established method for the design of macrocylic drugs, including peptidomimetic inhibitors for the cysteine protease calpain,[20,21] the HCV protease,[22] or the insulin-regulated aminopeptidase.[23] Therefore, the additional inhibitor **8** and its hydrogenated analogue **9** were synthesized by metathesis between *O*-allyl protected tyrosine residues. A cleavage of the *O*-alkyl bond during the hydrogenation in ethyl acetate was not observed (Scheme 2).

There exist several examples for the preparation of cyclized peptidomimetics using a copper-catalyzed azide alkyne cycloaddition (CuAAC,[24] also known as the copper-catalyzed Huisgen cycloaddition).[25,26] Therefore, a third cyclization strategy via click chemistry by reaction of the bis-propargylglycine intermediate **21** with various bis-azide derivatives was used for the synthesis of inhibitors **10**–**12**, which led to the formation of rigid triazole rings in the P2 and P3 side chains (Scheme 3).

dx.doi.org/10.1021/jm2011996 | *J. Med. Chem.* 2012, 55, 1171–1180

Scheme 2. Synthesis of Inhibitor 9[a]

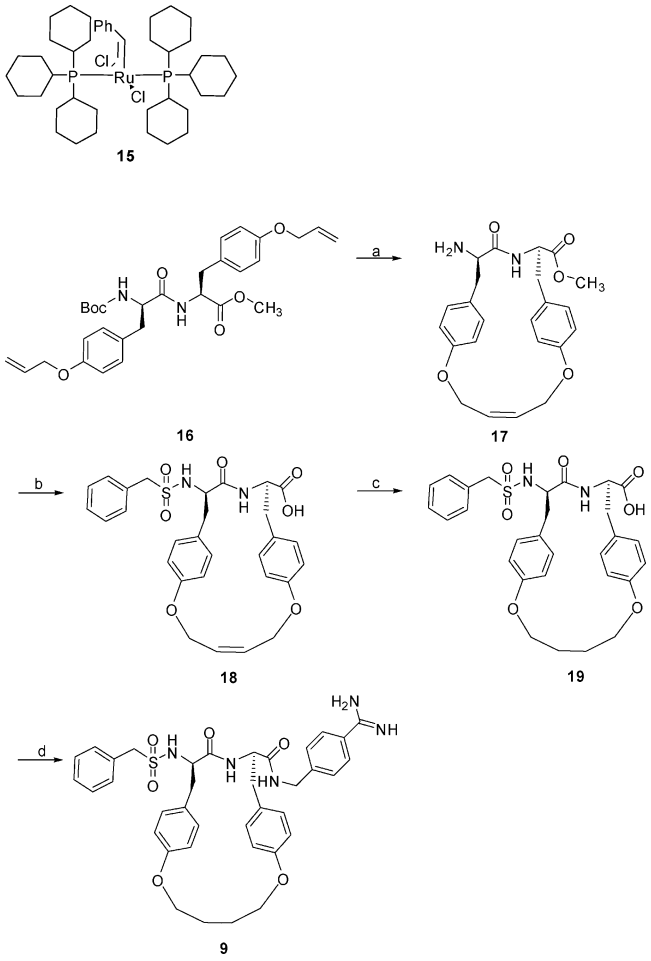

[a](a) (i) 0.05 equiv of Grubbs I **15**, DCM, reflux; (ii) 5 equiv of 1 N HCl/AcOH, room temp, preparative HPLC, 28% yield; (b) (i) 3 equiv of Bzls-Cl, MeCN/water, pH 7−8; (ii) 19 equiv of 1 N NaOH, 1,4-dioxane/water, 40 °C, 96% yield (two steps); (c) 10% Pd/C, EtOAc, room temp, 73% yield; (d) 1.2 equiv of 4-Amba·2HCl, 1.2 equiv of PyBOP, 2 equiv of DIPEA, DMF, 0 °C, preparative HPLC, 70% yield.

Scheme 3. Synthesis of Inhibitor 10[a]

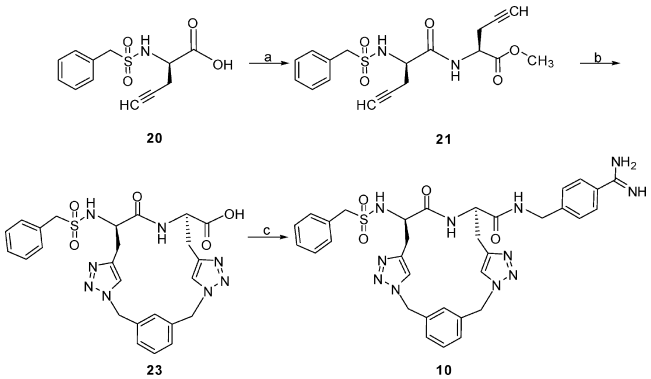

[a](a) 1 equiv of **20**, 1 equiv of H-Ppg-OMe·HCl, 1.1 equiv of PyBOP, 3 equiv of DIPEA, DMF, 0 °C; (b) (i) 1 equiv of 1,3-bis(azidomethyl)-benzene, 0.4 equiv of CuBr, 6 equiv of DIPEA, DMF/water, microwave (120 °C, 5 min, 150 W); (ii) 9 equiv of 1 N NaOH, DMF, room temp, 32% yield (two steps); (c) 1 equiv of isobutyl chloroformate, 2 equiv of NMM, 1.5 equiv of 4-Amba·2 HCl, DMF, −20 °C, preparative HPLC, 64% yield.

The structures of the synthesized cyclic inhibitors are summarized in Table 1.

Kinetic Measurements. A relatively weak inhibitory effect against plasmin (K_i = 431 nM) was obtained for compound **2**, in which two glutamic acid side chains were cyclized by amide bond formation with *m*-diaminoxylene. For comparison, we also determined the inhibition constants against the related trypsin-like serine proteases PK, thrombin, factor Xa, and aPC. All K_i values were obtained from Dixon plots and are summarized in Table 2.

Because of the higher potency found for the linear reference inhibitor **1**, which contains aromatic amino acid residues in P2 and P3 positions, we assumed that it might be beneficial to replace the flexible Glu residues by more hydrophobic and rigid amino acids. Therefore, inhibitors **3**−**7** containing the aromatic 3- or 4-aminomethylphenylalanine as P2 and/or P3 residues were designed, which could be cyclized using *p*- and *m*-phenylene or piperazinediacetic acid. Analogue **3** was already a significantly more potent and selective plasmin inhibitor compared to **2**, whereas its better soluble piperazine analogue **4** has a similar specificity profile. Both analogues inhibit plasmin with K_i < 10 nM. The plasmin inhibition could be further enhanced in the cases of compounds **5**−**7**, although inhibitors **6** and **7** possess reduced selectivity and inhibit various other proteases with inhibition constants of <50 nM. Especially, the potent inhibition of the clotting proteases thrombin and factor Xa, which are the physiological antagonists of the fibrinolytic plasmin, could be a disadvantage.

An improved selectivity was determined for compounds **8** and **9**, obtained by metathesis. Similar to aprotinin, both analogues retained some affinity against PK with inhibition constants of <20 nM. It is noted that PK contains only a glycine residue in position 99 (Figure 1). Most likely, its less demanding 99-loop (Figure 2) leads to a reduced repulsion from the cyclic ring structures of these inhibitors. Compounds **8** and **9** maintain high plasmin affinity with K_i < 3 nM. This is an additional hint that the incorporation of hydrophobic phenyl groups in the P2 and P3 side chains contributes to improved plasmin binding.

The third cyclization strategy via click chemistry provided the bis-triazole inhibitors **10**−**12**. Of particular interest might be the highly potent inhibitor **10** (K_i for plasmin of 0.77 nM), which is a relatively weak inhibitor of thrombin, factor Xa, and aPC. Its additional inhibitory effect on PK could also reduce the liberation of bradykinin from high-molecular-weight kininogen, which might result in a beneficial anti-inflammatory effect. This was also discussed as an advantage of aprotinin (K_i for PK of 30 nM) compared to other antifibrinolytic drugs, such as tranexamic acid, which has no inhibitory effect against PK.[27,28]

Docking of Inhibitor 10 in Plasmin. Because of its high potency, inhibitor **10** was docked using FlexX into the active site of plasmin to get an impression of its potential binding mode. The coordinates of the protease domain of plasmin were taken from the PDB entry 1bui.[8] The shown structure of inhibitor **10** (Figure 5) was selected based on similar backbone interactions known from related complexes of noncyclized substrate analogue inhibitors, e.g., with thrombin,[29,30] factor Xa,[19] factor VIIa,[31] trypsin,[32] or urokinase.[18]

The benzamidine forms the characteristic salt bridge to Asp189 and hydrogen-bonds to the carbonyl of Gly219 and the side chain oxygen of Ser190, whereas the amide NH of the P1 residue binds to the carbonyl oxygen of Ser214. However, in contrast to the noncyclized inhibitors only one hydrogen bond

dx.doi.org/10.1021/jm2011996 | J. Med. Chem. 2012, 55, 1171−1180

Table 1. Structures of the Synthesized Cyclic Inhibitors[a]

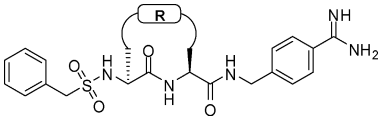

No.	R
2	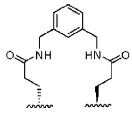
3	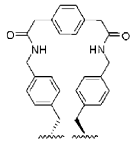
4	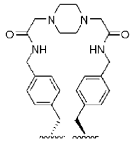
5	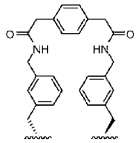
6	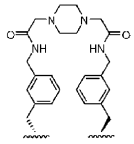
7	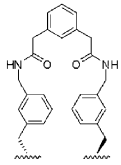
8*	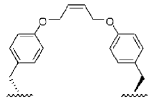
9	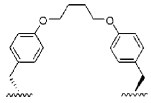
10	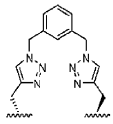
11	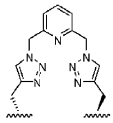
12	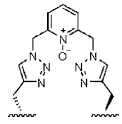

[a]The asterisk (*) indicates that this inhibitor was obtained as a 1:2.1 (*E*/*Z*) mixture.

Table 2. Inhibition of Plasmin and Related Trypsin-like Serine Proteases

	K_i (nM)				
compd	plasmin	PK	thrombin	FXa	aPC
1	0.81	0.075	667	42	0.61
2	431	25.4	2020	3430	5.1
3	9.4	868	6520	9370	12000
4	9.0	493	3517	3472	3510
5	6.9	136	45.4	152	564
6	4.1	25.3	7.2	21	48
7	1.1	17.4	26.8	42	223
8	2.5	9.4	137	220	90
9	1.1	19	510	784	4586
10	0.77	2.4	9490	206	3000
11	2.2	10.1	6175	1860	8390
12	8.9	67	1180	3123	>6000

is formed between the P3 backbone and Gly216. It seems that the rigid cyclic structure prohibits the formation of the second H-bond to the carbonyl oxygen of Gly216. Many docking solutions were found with very similar conformations of the P3−P2 ring structure, whereas the binding mode of the P4 benzylsulfonyl group seems to be more flexible. The sulfonyl group of inhibitor **10** in the selected conformation is H-bonded to the side chain of Gln192, which is additionally involved in an interaction with the P2 carbonyl group. As expected, the triazole rings and the phenyl linker between the P2 and P3 side chains are directed toward the large open binding pocket of plasmin. One triazole is located above the indole of Trp215, and the second is placed nearly parallel to the imidazole of His57, whereas the phenyl group is perpendicularly oriented between both triazole rings.

The shown complex was also overlaid with the structures of the other tested proteases. This resulted in a steric clash with thrombin, factor Xa, and aPC, whereas the selected inhibitor conformation seems to be well accepted in PK (see Figures S1−S4 in Supporting Information). These results confirm the found selectivity profile of inhibitor **10**.

DISCUSSION

By use of different cyclization strategies, it was possible to develop highly potent plasmin inhibitors with inhibition constants of <3 nM. The described cyclization between neighboring residues (*i* to *i* + 1) was possible because of the different configurations of the P2 and P3 amino acids in this substrate-analogue inhibitor type. This is quite different from most other cyclized peptidomimetics consisting only of L-amino acids, where the cyclization is often performed between the side chains of an amino acid *i* and a residue in the third position (*i* + 2)[20−22,33] or between residues that are further away in the peptide sequence. However, there also exist examples of a cyclization between neighboring side chains, e.g., of several 14-membered cycloisodityrosine derivatives, which were introduced in peptide antibiotics with antitumor activity, prepared by an Ullmann closure.[34−36]

The first cyclic inhibitor **2**, obtained by connecting two flexible glutamate side chains, had relatively weak potency, missing any selectivity. In contrast, the replacement of the glutamates by substituted phenylalanines immediately provided compounds with enhanced potency and selectivity. Especially, inhibitors **3** and **4** containing the largest 26-membered ring structures possess a weak affinity against the other tested

dx.doi.org/10.1021/jm2011996 | J. Med. Chem. 2012, 55, 1171−1180

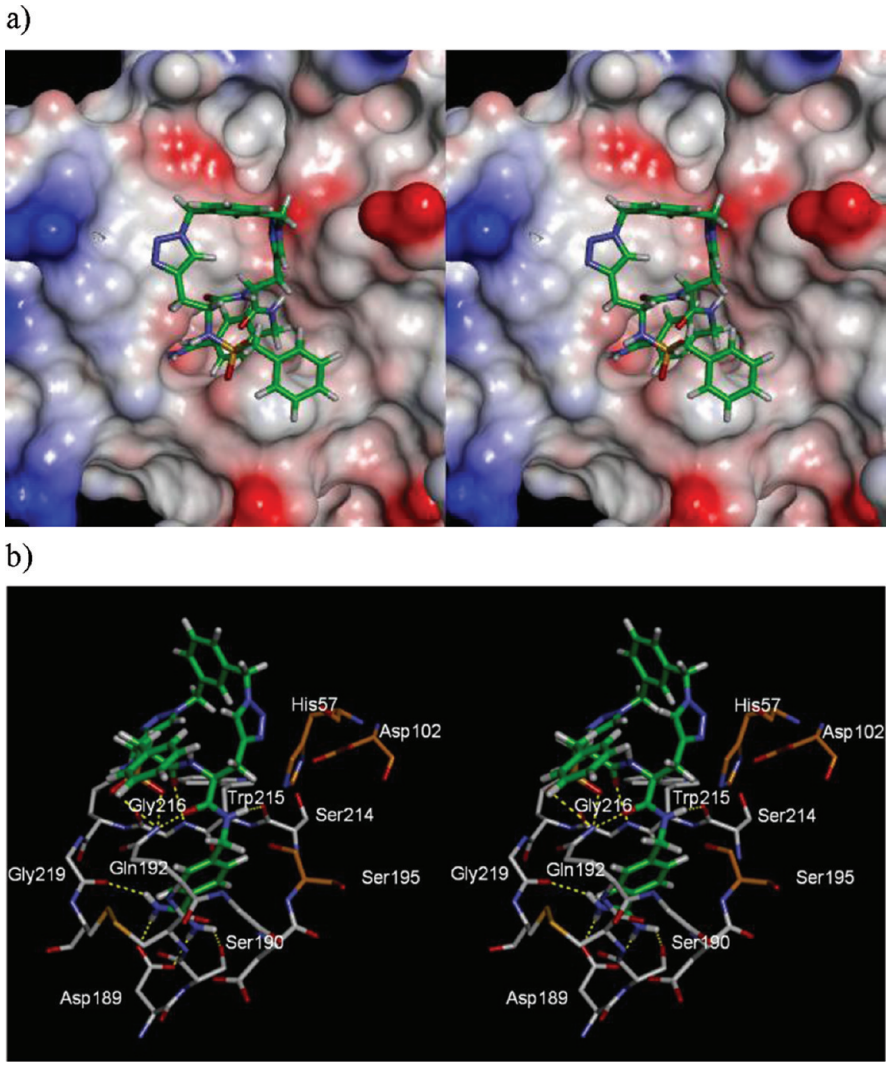

Figure 5. Stereoview of the modeled structure of inhibitor **10** (with green carbon atoms) in plasmin. (a) Part a shows the plasmin in surface representation for visualization of the overall binding mode. (b) Part b indicates the found binding interactions as yellow dashed lines. The residues of the catalytic triad are provided with orange carbon atoms.

proteases. Reduction of the ring size to 24 atoms (**5**, **6**) or 23 atoms (**7**) enhanced the affinity toward all enzymes but reduced the selectivity. Further downsizing the cycle in the cases of inhibitors **8** and **9** to 20 atoms, prepared by ring closure metathesis, maintained the high potency as plasmin inhibitors with K_i < 3 nM. A noncyclized analogue benzylsulfonyl-D-Tyr(All)-Tyr(All)-4-amidinobenzylamide has a significantly reduced inhibitory potency against plasmin with an inhibition constant of 65 nM. Therefore, we assume that a significant contribution for the enhanced binding affinity is caused by the rigidization of the inhibitor conformation in solution, resulting in a beneficial entropic effect during binding to plasmin. The smallest 17-membered ring containing compounds were prepared by click chemistry, whereas analogues **10** and **11** were found to be excellent plasmin inhibitors with K_i of 0.77 and 2.2 nM, respectively. Both compounds are also relatively potent PK inhibitors with inhibition constants of ≤10 nM, whereas they have weak affinity for thrombin, factor Xa, or aPC. However, these kinetic data indicate that there is obviously no simple correlation between the ring size of the inhibitors and their inhibitory potency or selectivity.

The high plasmin affinity obtained for several analogues demonstrates that the cyclization also can compensate for the loss of the important guanidinomethyl group present in the P2 side chain of the linear analogue **1**, which is most likely involved in a salt bridge to the plasmin residue Glu60 (Figure 4). The docking experiments exemplarily performed with compound **10** revealed that the inhibitor adopts a very compact and rigid structure, which still enables an efficient binding to the open active site of plasmin, whereas it decreases the affinity for thrombin, factor Xa, and aPC.

■ CONCLUSION

These cyclized inhibitors might be of potential interest for the development of novel antifibrinolytics. Some compounds were found to be very selective plasmin inhibitors, while others additionally inhibit PK with $K_i \leq 10$ nM. An inhibitory effect on PK could be an advantage for reducing systemic inflammatory processes, which often occur in cardiac surgery with cardiopulmonary bypass that requires antifibrinolytic therapy. An additional application could be the use of these compounds as antidote to reduce excessive bleeding during fibrinolytic therapy with plasmin[37] or plasminogen activators. Without any doubt

dx.doi.org/10.1021/jm2011996 | J. Med. Chem. 2012, 55, 1171−1180

there may exist many alternative cyclization possibilities between the P2 and P3 residues, as long as their side chains contain suitable groups for coupling, either directly or with appropriate linker segments. The strong potency and relatively high selectivity found for these first analogues confirm that this cyclization strategy provides a new access to excellent substrate-analogue plasmin inhibitors.

EXPERIMENTAL SECTION

Analytical HPLC experiments were performed on a Shimadzu LC-10A system (column, Nucleodur C_{18}, 5 μm, 100 Å, 4.6 mm × 250 mm, Machery-Nagel, Düren, Germany) with a linear gradient of acetonitrile (1%/min increase in concentration of acetonitrile, detection at 220 nm) containing 0.1% TFA at a flow rate of 1 mL/min. The final inhibitors were purified to more than 95% purity (detection at 220 nm) by preparative HPLC using a Varian PrepStar model 218 gradient system (column, Nucleodur, 5 μm, 100 Å, 32 mm × 250 mm, Macherey-Nagel, Düren, Germany) and a linear gradient of acetonitrile containing 0.1% TFA at a flow rate of 20 mL/min. All inhibitors were finally obtained as TFA salts after lyophilization. The molecular masses were determined using a QTrap 2000 ESI spectrometer (Applied Biosystems). The ^{1}H and ^{13}C NMR spectra were recorded on a ECX-400 (Jeol Inc., U.S.) and are referenced to internal solvent signals.

Boc-D-Tyr(All)-Tyr(All)-OMe (16). Boc-D-Tyr(All)-OH (2 g, 6.22 mmol, 1.0 equiv) and H-Tyr(All)-OMe (1.7 g, 6.22 mmol, 1.0 equiv) were dissolved in 50 mL of DMF and stirred on the ice bath. After the addition of HBTU (2.36 g, 6.22 mmol, 1.0 equiv) and DIPEA (3.25 mL, 18.7 mmol, 3.0 equiv), the solution was stirred for 2 h. The solvent was removed in vacuo, and the remaining residue was dissolved in a mixture of a 5% $KHSO_4$ and ethyl acetate. The organic phase was washed thrice with 5% $KHSO_4$, once with brine, thrice with saturated aqueous $NaHCO_3$, and thrice with brine, dried over Na_2SO_4, and filtered and the solvent removed in vacuo. Yield: 3.32 g (6.16 mmol, 99.1%) as a yellow amorphous solid. HPLC: 52.1 min, start at 10% B (purity, 96.9%). ^{1}H NMR (DMSO-d_6, 400 MHz): δ = 8.36 (d, J = 8.1 Hz, 1 H), 7.09 (d, J = 8.5 Hz, 2 H), 7.00 (d, J = 8.5 Hz, 2 H), 6.80 (d, J = 8.7 Hz, 2 H), 6.77 (d, J = 8.6 Hz, 2 H), 6.67 (d, J = 8.8 Hz, 1 H), 5.87−6.05 (m, 2 H), 5.12−5.38 (m, 4 H), 4.43−4.49 (m, 4 H), 3.60 (s, 3 H), 2.95 (dd, J = 13.7, 5.1 Hz, 2 H), 2.77 (dd, J = 13.8, 9.5 Hz, 2 H), 2.65 (s, 1 H), 2.59 (dd, J = 13.8, 3.9 Hz, 1 H), 1.25 ppm (s, 9 H). ^{13}C NMR (DMSO-d_6, 101 MHz): δ = 172.0, 171.7, 156.9, 156.7, 155.1, 133.9, 133.7, 130.1, 129.0, 117.2, 114.4, 114.1, 77.9, 68.1, 55.5, 53.5, 51.9, 36.7, 36.2, 28.1 ppm. MS (ESI, positive): calcd, 538.27; m/z, 539.5 $[M + H]^+$, 561.5 $[M + Na]^+$, 1099 $[2M + Na]^+$.

Intermediate 17. Boc-D-Tyr(All)-Tyr(All)-OMe (500 mg, 0.928 mmol, 1.0 equiv) was dissolved in 250 mL of dry DCM under an atmosphere of argon, which was degassed before 30 min using ultrasound. The mixture was flushed with argon on a water bath at 40 °C for an additional 30 min. After the addition of Grubbs I catalyst (38 mg, 0.0464 mmol, 0.05 equiv), dissolved in 10 mL of degassed DCM, the mixture was refluxed under an atmosphere of argon for 6 h and stirred at room temperature overnight. The solvent was removed in vacuo, and the dark red residue was dissolved in 40 mL of acetone, adsorbed onto a small amount of silica gel 60, and evaporated. The product was purified on silica gel 60 (column 3 cm × 40 cm) using isohexane/TMBE (1/1, v/v) as eluent. The product containing fractions were combined, and the solvent was evaporated. Yield: 310 mg (0.6068 mmol, 65.4%) as a white solid. HPLC: 43.3 min, start at 10% B (purity, 59.2%). The white solid (294 mg, 0.575 mmol, 1.0 equiv) was dissolved in 575 μL of acetic acid and 2.9 mL of 1 N HCl in AcOH. After 1 h, the solvent was removed in vacuo and the remaining light yellow residue was dissolved in 40% solvent B and purified by preparative HPLC (C_{18} column, start at 25% B). The product containing fractions were combined and lyophilized. Yield: 136.4 mg (0.260 mmol, 28.0%) of a white lyophilized solid. HPLC: 30.7 min, start at 10% B (95.1%). MS (ESI, positive): calcd, 410.18; m/z, 411.06 $[M + H]^+$, 821.30 $[2M + H]^+$.

Intermediate 18. 17 (136 mg, 0.260 mmol, 1.0 equiv) was dissolved in 10 mL of MeCN and 3 mL of water. Then Bzls-Cl (148.3 mg, 0.778 mmol, 3.0 equiv) was added in several portions, and the pH was adjusted with 1 N NaOH to 7−8. The solvent was removed in vacuo after 4.5 h. The remaining residue was dissolved in 10 mL of 1,4-dioxane and 5 mL of water and treated with 5 mL of 1 N NaOH. The mixture was stirred at 40 °C on the water bath for 1 h. The solution was neutralized by addition of TFA, and the solvent was removed in vacuo. The remaining residue was dissolved in a mixture of 5% $KHSO_4$ and ethyl acetate, and the water layers were extracted thrice with ethyl acetate. The combined organic phases were washed twice with 5% $KHSO_4$ and thrice with brine, dried over Na_2SO_4, and filtered, and the solvent was removed in vacuo. Yield: 138 mg (0.251 mmol, 96.4%) of a white amorphous solid. HPLC: 45.8 min, start at 10% B (76.2%). MS (ESI, positive): calcd, 550.18; m/z, 551.5 $[M + H]^+$, 573.5 $[M + Na]^+$, 589.4 $[M + K]^+$.

Intermediate 19. 18 (55 mg, 0.0999 mmol) was dissolved in 110 mL of ethyl acetate. After the addition of 5.8 mg of 10% Pd/C, the mixture was hydrogenated at room temperature for 3 h. The catalyst was removed by filtration, and the solvent was evaporated. Yield: 40 mg (0.0724 mmol, 72.5%) of a light gray amorphous solid. HPLC: 19.7 min, start at 40% B (purity, 95.9%). MS (ESI, positive): calcd, 552.19; m/z, 553.10 $[M + H]^+$, 570.09 $[M + NH_4]^+$.

Inhibitor 9. 19 (30 mg, 0.0543 mmol, 1.0 equiv) and 4-amidinobenzylamine·2 HCl (14.5 mg, 0.0663 mmol, 1.2 equiv) were suspended in 10 mL of DMF and stirred on an ice bath. The mixture was treated with PyBOP (33.8 mg, 0.0654 mmol, 1.2 equiv) and DIPEA (18.8 μL, 0.109 mmol, 2.0 equiv) and was stirred at room temperature overnight. The solvent was removed in vacuo, and the remaining residue was dissolved in 50% solvent B and filtered through a 0.2 μm membrane filter. The filtrate was purified by preparative HPLC (C_{18} column, start at 35% B). The product containing fractions were combined and lyophilized. Yield: 30.1 mg (0.0377 mmol, 69.5%) of a white lyophilized solid. HPLC: 13.9 min, start at 40% B (purity, 100.0%). ^{1}H NMR (DMSO-d_6, 400 MHz): δ = 9.21 (br s, 2 H), 8.97 (br s, 2 H), 8.64 (t, J = 6.0 Hz, 1 H), 8.47 (d, J = 6.9 Hz, 1 H), 7.70 (d, J = 8.3 Hz, 2 H), 7.58 (d, J = 8.2 Hz, 1 H), 7.43 (d, J = 8.2 Hz, 2 H), 7.25−7.39 (m, 5 H), 6.88 (d, J = 8.5 Hz, 2 H), 6.77 (d, J = 8.5 Hz, 2 H), 6.59 (d, J = 8.5 Hz, 2 H), 6.49 (d, J = 8.5 Hz, 2 H), 4.38−4.49 (m, 2 H), 4.30−4.38 (m, 2 H), 4.21−4.29 (m, 2 H), 4.07−4.14 (m, 2 H), 3.96−4.06 (m, 2 H), 2.76−2.87 (m, 2 H), 2.63−2.73 (m, 2 H), 1.72−1.92 ppm (m, 4 H). MS (ESI, positive): calcd, 683.82; m/z, 684.43 $[M + H]^+$. TLC: R_f = 0.79.

Bzls-D-Ppg-OH (20). H-D-Ppg-OH·HCl (500 mg, 3.34 mmol, 1.0 equiv) was suspended in 10 mL of dry DCM and treated with TMS-Cl (912 μL, 7.35 mmol, 2.2 equiv) and DIPEA (1.861 mL, 10.7 mmol, 3.2 equiv). The mixture was refluxed for 1 h. Then benzylsulfonyl chloride (705 mg, 3.70 mmol, 1.1 equiv) was added in several portions within 35 min at 0 °C and the pH was maintained at 8−9 by addition of DIPEA (700 μL, 4.02 mmol, 1.2 equiv). The mixture was stirred 1 h at 0 °C and at room temperature overnight. The solvent was removed in vacuo, and the brown residue was dissolved in water and the pH adjusted to 8−9 with 1 N NaOH. The solution was extracted twice with EtOAc. The organic phases were discarded. The aqueous layer was adjusted to pH 1 with 5% $KHSO_4$ and extracted thrice with EtOAc. The combined organic phase was washed twice with 5% $KHSO_4$ and twice with brine. The organic layers were dried over Na_2SO_4 and filtered, and the solvent was removed in vacuo. Yield: 481 mg (1.80 mmol, 53.8%) of a brown oil. HPLC: 26.7 min, start at 10% B (purity, 81.0%). ^{1}H NMR (DMSO-d_6, 400 MHz): δ = 13.06 (br s, 1 H), 7.61 (d, J = 8.3 Hz, 1 H), 7.27−7.43 (m, 5 H), 4.28−4.40 (m, 2 H), 3.93 (dt, J = 8.1, 6.5 Hz, 1 H), 2.92 (t, J = 2.6 Hz, 1 H), 2.48−2.52 ppm (m, 2 H). ^{13}C NMR (DMSO-d_6, 101 MHz): δ = 171.7, 131.0, 130.1, 128.3, 128.1, 80.1, 73.6, 58.7, 54.8, 22.8 ppm. MS (ESI, positive): calcd, 267.06; m/z, 285 $[M + NH_4]^+$, 290 $[M + Na]^+$.

Bzls-D-Ppg-Ppg-OMe (21). 20 (473 mg, 1.77 mmol, 1.0 equiv) and H-Ppg-OMe·HCl (292 mg, 1.79 mmol, 1.0 equiv) were dissolved in 23.5 mL of DMF and treated with PyBOP (1.02 g, 1.96 mmol, 1.1 equiv) and DIPEA (928 μL, 5.33 mmol, 3.0 equiv) at 0 °C, pH 8−9. The mixture was stirred for 30 min at 0 °C and at room temperature

dx.doi.org/10.1021/jm2011996 | J. Med. Chem. 2012, 55, 1171−1180

overnight. The solvent was removed in vacuo, and the remaining residue was dissolved in EtOAc. The organic phase was washed thrice with solutions of 5% $KHSO_4$, once with brine, thrice with saturated aqueous $NaHCO_3$, and thrice with brine. The organic phase was dried over Na_2SO_4 and filtered. The solvent was removed in vacuo, and the product was crystallized from EtOAc. Yield: 236.7 mg (0.629 mmol, 35.5%) of a beige solid. HPLC: 35.6 min, start at 10% B (purity, 96.2%). ^{1}H NMR (DMSO-d_6, 400 MHz): δ = 8.83 (d, J = 7.7 Hz, 1 H), 7.67 (d, J = 8.8 Hz, 1 H), 7.32−7.41 (m, 5 H), 4.50 (q, J = 7.5 Hz, 1 H), 4.29 (d, J = 8.6 Hz, 2 H), 4.14 (q, J = 7.5 Hz, 1 H), 3.63 (s, 3 H), 2.98−3.06 (m, 1 H), 2.88−2.95 (m, 2 H), 2.64 (dd, J = 6.7, 2.3 Hz, 2 H), 1.73 ppm (s, 1 H). ^{13}C NMR (DMSO-d_6, 101 MHz): δ = 170.4, 169.8, 130.8, 130.0, 128.2, 127.9, 80.0, 79.6, 73.4, 58.6, 54.9, 52.2, 51.1, 23.3, 21.0 ppm. MS (ESI, positive): calcd, 376,11; m/z, 399 $[M + Na]^+$, 775 $[2M + Na]^+$.

1,3-Bis(azidomethyl)benzene (22). The synthesis was previously described by Ramírez-López et al.[38] α,α-Dibromo-m-xylene (1.32 g, 5.0 mmol, 1.0 equiv) was dissolved in 30 mL of DMSO and treated with sodium azide (810 mg, 12.5 mmol, 2.5 equiv). The mixture was stirred for 2 h at room temperature. The yellow solution was quenched with ice−water and extracted thrice with EtOAc. The combined organic layers were washed twice with water and once with brine, dried over Na_2SO_4, filtered, and the solvent was removed in vacuo. Yield: 880 mg (4.68 mmol, 93.5%) of a yellow oil. HPLC: 20.8 min, start at 40% B (purity, 96.0%). MS (EI): calcd, 188.08; m/z (%), 188 $[M]^+$ (100), 146 $[M - N_3]^+$ (61), 104 $[M - N_6]^+$ (25), 91 $[M - CH_2 - N_6]^+$ (25), 77 $[M - C_2H_4 - N_6]^+$ (21), 118 $[M - N_5]^+$ (19), 189 $[M + H]^+$ (14), 117 $[C_8H_7N]^+$ (13), 78 $[C_6H_6]^+$ (12), 131 $[C_8H_7N_2]^+$ (11), 147 $[C_8H_9N_3]^+$ (8), 105 $[C_8H_9]^+$ (6).

Intermediate 23. **21** (150 mg, 0.399 mmol, 1.0 equiv), 1,3-bis(azidomethyl)benzene **22** (63 mg, 0.399 mmol, 1.0 equiv), and CuBr (23 mg, 0.159 mmol, 0.4 equiv) were dissolved in 50 mL of DMF and 1 mL of water by addition of DIPEA (416 μL, 2.39 mmol, 6.0 equiv). The reaction was performed at 120 °C in a microwave (Discover, CEM) for 5 min at 150 W (temperature priority). The solvent was removed in vacuo, and the methyl ester was obtained as a crude product. A small sample was purified by preparative HPLC for NMR analysis. Oil. HPLC: 13.3 min, start at 30% B. MS (ESI, positive): calcd, 564.19; m/z, 565.12 $[M + H]^+$. ^{1}H NMR (DMSO-d_6, 500 MHz): δ = 8.56 (d, J = 6.9 Hz, 1 H), 7.79 (s, 1 H), 7.74 (d, J = 8.9 Hz, 1 H), 7.61 (s, 1 H), 7.40−7.47 (m, 5 H), 7.33−7.40 (m, 3 H), 6.39 (s, 1 H), 5.57 (d, J = 5.0 Hz, 2 H), 5.49 (s, 2 H), 4.55 (d, J = 13.7 Hz, 1 H), 4.47 (t, J = 7.5 Hz, 1 H), 4.31 (d, J = 13.7 Hz, 1 H), 4.23 (t, J = 8.2 Hz, 1 H), 3.64 (s, 3 H), 3.18 (dd, J = 14.3, 10.9 Hz, 1 H), 3.08 (dd, J = 15.4, 2.0 Hz, 1 H), 2.98 (dd, J = 15.1, 11.0 Hz, 1 H), 2.82 ppm (dd, J = 14.3, 2.6 Hz, 1 H). This procedure was repeated twice. The combined products of these three reactions were dissolved in 30 mL of DMF and treated with 3.6 mL of 1 N NaOH. The mixture was stirred for 1 h at room temperature. The solvent was removed in vacuo. The residue was suspended in a mixture of EtOAc and 5% $KHSO_4$. The water phase was extracted twice with EtOAc. The combined organic phases were washed once with 5% $KHSO_4$, thrice with brine, dried over Na_2SO_4, and filtered, and the solvent was removed in vacuo. Yield: 208 mg (0.378 mmol, 31.6%) of a slightly yellow, amorphous solid. HPLC: 18.5 min, start at 20% B (purity, 85.3%). MS (ESI, positive): calcd, 550.17; m/z, 551.22 $[M + H]^+$, 573.12 $[M + Na]^+$.

Inhibitor 10. **23** (98 mg, 0.178 mmol, 1.0 equiv) and NMM (19.6 μL, 0.178 mmol, 1.0 equiv) were dissolved in 5 mL of DMF at −20 °C and treated with isobutyl chloroformate (23.1 μL, 0.178 mmol, 1.0 equiv). The mixture was stirred for 10 min at −15 °C and treated with 4-amidinobenzylamine·2HCl (59.3 mg, 0.267 mmol, 1.5 equiv) and NMM (19.6 μL, 0.178 mmol, 1.0 equiv). The suspension was stirred at −20 °C for an additional hour and at room temperature overnight. The solvent was removed in vacuo. The remaining slightly yellow residue was dissolved in 35% solvent B and purified by preparative HPLC (C_{18} column, start of the gradient at 20% B). The product containing fractions were combined, and the solvent was partially removed in vacuo, followed by lyophilization of the product. Yield: 78 mg (0.114 mmol, 64.3%) white lyophilized solid. HPLC: 24.7 min, start at 10% B (purity, 96.1%). ^{1}H NMR (DMSO-d_6, 500 MHz): δ = 9.20 (br s, 2 H), 9.04 (br s, 2 H), 8.55 (t, J = 5.9 Hz, 1 H), 8.36 (d, J = 6.9 Hz, 1 H), 7.70 (d, J = 8.3 Hz, 2 H), 7.64 (d, J = 8.9 Hz, 2 H), 7.60 (s, 1 H), 7.37−7.46 (m, 5 H), 7.33−7.37 (m, 2 H), 7.28−7.31 (m, 3 H), 6.33 (s, 1 H), 5.51−5.57 (m, 2 H), 5.45−5.51 (m, 2 H), 4.49 (d, J = 13.7 Hz, 1 H), 4.38−4.43 (m, 1 H), 4.34 (d, J = 12.9 Hz, 3 H), 4.24−4.29 (m, 1 H), 3.16 (dd, J = 14.7, 10.5 Hz, 2 H), 2.95−3.03 ppm (m, 2 H). ^{13}C NMR (DMSO-d_6, 126 MHz): δ = 171.2, 170.3, 165.4, 145.7, 143.5, 142.1, 137.1, 137.1, 130.9, 130.1, 128.8, 128.2, 128.1, 128.0, 127.4, 127.3, 127.3, 126.4, 124.4, 123.0, 122.6, 58.2, 55.1, 54.0, 52.2, 52.2, 41.8, 29.3, 27.9 ppm. MS (ESI, positive): calcd, 681.26; m/z, 341.58 $[2M + H]^{2+}/2$, 682.08 $[M + H]^+$. TLC: R_f = 0.43.

Molecular Modeling. *Preparation of Plasmin.* For the docking process, we only used the coordinates of the protease domain of plasmin taken from the microplasmin−staphylokinase−microplasmin ternary complex irreversibly inhibited by H-Glu-Gly-Arg-chloromethyl ketone (PDB entry 1bui). All water molecules and the covalent bonds of the inhibitor to the plasmin residues His57 and Ser195 were deleted, followed by addition of hydrogens and calculation of partial charges (Gasteiger and Marsili) using SYBYL.[39]

Inhibitor Preparation and Docking. Ligand **10** was prepared using the MOE builder function. For the docking process various conformers of the inhibitor[40] were used, which were generated using the conformational search function of MOE[41] (conformational search using LowModeMD[42] and MM Iteration Limit 1000; all other standard parameters were set on default). These conformers were docked using FlexX.[43] The active site of plasmin was defined by taking all residues within 10 Å around H-Glu-Gly-Arg-chloromethyl ketone, taken from the crystal structure. The 100 top-scoring poses were retained and thoroughly inspected.

■ ASSOCIATED CONTENT

Ⓢ Supporting Information

Synthesis procedures for all other inhibitors and analytical data, information for enzyme kinetics, and also figures of the modeled plasmin/inhibitor **10** complex overlaid with the X-ray structures of the other tested proteases. This material is available free of charge via the Internet at http://pubs.acs.org.

■ AUTHOR INFORMATION

Corresponding Author

*Phone: +49 6421 2825900. E-mail: steinmetzer@staff.uni-marburg.de.

■ ACKNOWLEDGMENTS

We thank Peter Steinmetzer and Sven Letschert from The Medicines Company (Leipzig) GmbH for K_i determinations. We also thank Gerhard Klebe for providing us access to the used modeling programs. Financial aid by The Medicines Company (Leipzig) GmbH is acknowledged.

■ ABBREVIATIONS USED

AcOH, acetic acid; 4-Amba, 4-amidinobenzylamine; Bzls-Cl, benzylsulfonyl chloride; DIPEA, *N*,*N*-diisopropylethylamine; EtOAc, ethyl acetate; NMM, 4-methylmorpholine; Ppg, propargylglycine; TMS-Cl, trimethylsilyl chloride

■ REFERENCES

(1) Mangano, D. T.; Tudor, I. C.; Dietzel, C.; G..; Ischemia, R.; Education, F. Multicenter study of perioperative ischemia research, the risk associated with aprotinin in cardiac surgery. *N. Engl. J. Med.* **2006**, *354*, 353−365.

(2) Straub, A.; Roehrig, S.; Hillisch, A. Oral, direct thrombin and factor Xa inhibitors: the replacement for warfarin, leeches, and pig intestines? *Angew. Chem., Int. Ed.* **2011**, *50*, 4574−4590.

(3) Okada, Y.; Tsuda, Y.; Tada, M.; Wanaka, K.; Okamoto, U.; Hijikata-Okunomiya, A.; Okamoto, S. Development of potent and selective plasmin and plasma kallikrein inhibitors and studies on the structure−activity relationship. *Chem. Pharm. Bull. (Tokyo)* **2000**, *48*, 1964−1972.
(4) Tsuda, Y.; Tada, M.; Wanaka, K.; Okamoto, U.; Hijikata-Okunomiya, A.; Okamoto, S.; Okad, Y. Structure−inhibitory activity relationship of plasmin and plasma kallikrein inhibitors. *Chem. Pharm. Bull. (Tokyo)* **2001**, *49*, 1457−1463.
(5) Xue, F.; Seto, C. T. Selective inhibitors of the serine protease plasmin: probing the S3 and S3′ subsites using a combinatorial library. *J. Med. Chem.* **2005**, *48*, 6908−6917.
(6) Xue, F.; Seto, C. T. Structure−activity studies of cyclic ketone inhibitors of the serine protease plasmin: design, synthesis, and biological activity. *Bioorg. Med. Chem.* **2006**, *14*, 8467−8487.
(7) Swedberg, J. E.; Harris, J. M. Plasmin substrate binding site cooperativity guides the design of potent peptide aldehyde inhibitors. *Biochemistry* **2011**, *50*, 8454−8462.
(8) Parry, M. A.; Fernandez-Catalan, C.; Bergner, A.; Huber, R.; Hopfner, K. P.; Schlott, B.; Guhrs, K. H.; Bode, W. The ternary microplasmin−staphylokinase−microplasmin complex is a proteinase−cofactor−substrate complex in action. *Nat. Struct. Biol.* **1998**, *5*, 917−923.
(9) Schechter, I.; Berger, A. On the size of the active site in proteases. I. Papain. *Biochem. Biophys. Res. Commun.* **1967**, *27*, 157−162.
(10) Schweinitz, A.; Stürzebecher, A.; Stürzebecher, U.; Schuster, O.; Stürzebecher, J.; Steinmetzer, T. New substrate analogue inhibitors of factor Xa containing 4-amidinobenzylamide as P1 residue: part 1. *Med Chem* **2006**, *2*, 349−361.
(11) Tang, J.; Yu, C. L.; Williams, S. R.; Springman, E.; Jeffery, D.; Sprengeler, P. A.; Estevez, A.; Sampang, J.; Shrader, W.; Spencer, J.; Young, W.; McGrath, M.; Katz, B. A. Expression, crystallization, and three-dimensional structure of the catalytic domain of human plasma kallikrein. *J. Biol. Chem.* **2005**, *280*, 41077−41089.
(12) The superposition of the structures and Figure 2 was created with the Discovery Studio Visualizer 3.0 from Accelrys Inc.
(13) Gustafsson, D.; Bylund, R.; Antonsson, T.; Nilsson, I.; Nystrom, J. E.; Eriksson, U.; Bredberg, U.; Teger-Nilsson, A. C. A new oral anticoagulant: the 50-year challenge. *Nat. Rev. Drug Discovery* **2004**, *3*, 649−659.
(14) Shiraishi, T.; Kadono, S.; Haramura, M.; Kodama, H.; Ono, Y.; Iikura, H.; Esaki, T.; Koga, T.; Hattori, K.; Watanabe, Y.; Sakamoto, A.; Yoshihashi, K.; Kitazawa, T.; Esaki, K.; Ohta, M.; Sato, H.; Kozono, T. Factor VIIa inhibitors: target hopping in the serine protease family using X-ray structure determination. *Bioorg. Med. Chem. Lett.* **2008**, *18*, 4533−4537.
(15) Tucker, T. J.; Lumma, W. C.; Mulichak, A. M.; Chen, Z.; Naylor-Olsen, A. M.; Lewis, S. D.; Lucas, R.; Freidinger, R. M.; Kuo, L. C. Design of highly potent noncovalent thrombin inhibitors that utilize a novel lipophilic binding pocket in the thrombin active site. *J. Med. Chem.* **1997**, *40*, 830−832.
(16) Schweinitz, A.; Steinmetzer, T.; Banke, I. J.; Arlt, M. J.; Stürzebecher, A.; Schuster, O.; Geissler, A.; Giersiefen, H.; Zeslawska, E.; Jacob, U.; Krüger, A.; Stürzebecher, J. Design of novel and selective inhibitors of urokinase-type plasminogen activator with improved pharmacokinetic properties for use as antimetastatic agents. *J. Biol. Chem.* **2004**, *279*, 33613−33622.
(17) Steinmetzer, T.; Schweinitz, A.; Stürzebecher, J.; Steinmetzer, P.; Söffing, A.; van de Locht, A.; Nicklisch, S.; Reichelt, C.; Ludwig, A.-F.; Schulze, A.; Daghisch, M.; Heinicke, J. Trypsin-like Serine Protease Inhibitors, and Their Preparation and Use. WO 2008/049595.
(18) Schweinitz, A.; Steinmetzer, T.; Banke, I. J.; Arlt, M. J.; Stürzebecher, A.; Schuster, O.; Geissler, A.; Giersiefen, H.; Zeslawska, E.; Jacob, U.; Kruger, A.; Stürzebecher, J. Design of novel and selective inhibitors of urokinase-type plasminogen activator with improved pharmacokinetic properties for use as antimetastatic agents. *J. Biol. Chem.* **2004**, *279*, 33613−33622.
(19) Schweinitz, A.; Stürzebecher, A.; Stürzebecher, U.; Schuster, O.; Stürzebecher, J.; Steinmetzer, T. New substrate analogue inhibitors of factor Xa containing 4-amidinobenzylamide as P1 residue: part 1. *Med. Chem.* **2006**, *2*, 349−361.
(20) Abell, A. D.; Jones, M. A.; Coxon, J. M.; Morton, J. D.; Aitken, S. G.; McNabb, S. B.; Lee, H. Y. Y.; Mehrtens, J. M.; Alexander, N. A.; Stuart, B. G.; Neffe, A. T.; Bickerstaffe, R. Molecular modeling, synthesis, and biological evaluation of macrocyclic calpain inhibitors. *Angew. Chem., Int. Ed.* **2009**, *48*, 1455−1458.
(21) Stuart, B. G.; Coxon, J. M.; Morton, J. D.; Abell, A. D.; McDonald, D. Q.; Aitken, S. G.; Jones, M. A.; Bickerstaffe, R. Molecular modeling: a search for a calpain inhibitor as a new treatment for cataractogenesis. *J. Med. Chem.* **2011**, *54*, 7503−7522.
(22) Liverton, N. J.; Holloway, M. K.; McCauley, J. A.; Rudd, M. T.; Butcher, J. W.; Carroll, S. S.; DiMuzio, J.; Fandozzi, C.; Gilbert, K. F.; Mao, S. S.; McIntyre, C. J.; Nguyen, K. T.; Romano, J. J.; Stahlhut, M.; Wan, B. L.; Olsen, D. B.; Vacca, J. P. Molecular modeling based approach to potent P2−P4 macrocyclic inhibitors of hepatitis C NS3/4A protease. *J. Am. Chem. Soc.* **2008**, *130*, 4607−4609.
(23) Andersson, H.; Demaegdt, H.; Johnsson, A.; Vauquelin, G.; Lindeberg, G.; Hallberg, M.; Erdelyi, M.; Karlen, A.; Hallberg, A. Potent macrocyclic inhibitors of insulin-regulated aminopeptidase (IRAP) by olefin ring-closing metathesis. *J. Med. Chem.* **2011**, *54*, 3779−3792.
(24) Pedersen, D. S.; Abell, A. 1,2,3-Triazoles in peptidomimetic chemistry. *Eur. J. Org. Chem.* **2011**, 2399−2411.
(25) Chen, J.; Nikolovska-Coleska, Z.; Yang, C. Y.; Gomez, C.; Gao, W.; Krajewski, K.; Jiang, S.; Roller, P.; Wang, S. Design and synthesis of a new, conformationally constrained, macrocyclic small-molecule inhibitor of STAT3 via "click chemistry". *Bioorg. Med. Chem. Lett.* **2007**, *17*, 3939−3942.
(26) Cantel, S.; Le Chevalier Isaad, A.; Scrima, M.; Levy, J. J.; DiMarchi, R. D.; Rovero, P.; Halperin, J. A.; D'Ursi, A. M.; Papini, A. M.; Chorev, M. Synthesis and conformational analysis of a cyclic peptide obtained via *i* to *i* + 4 intramolecular side-chain to side-chain azide-alkyne 1,3-dipolar cycloaddition. *J. Org. Chem.* **2008**, *73*, 5663−5674.
(27) Lazar, H. L.; Bao, Y.; Tanzillo, L.; O'Gara, P.; Reardon, D.; Price, D.; Crowley, R.; Cabral, H. J. Aprotinin decreases ischemic damage during coronary revascularization. *J. Card. Surg.* **2005**, *20*, 519−523.
(28) Engles, L. Review and application of serine protease inhibition in coronary artery bypass graft surgery. *Am. J. Health-Syst. Pharm.* **2005**, *62*, S9−14.
(29) Stauffer, K. J.; Williams, P. D.; Selnick, H. G.; Nantermet, P. G.; Newton, C. L.; Homnick, C. F.; Zrada, M. M.; Lewis, S. D.; Lucas, B. J.; Krueger, J. A.; Pietrak, B. L.; Lyle, E. A.; Singh, R.; Miller-Stein, C.; White, R. B.; Wong, B.; Wallace, A. A.; Sitko, G. R.; Cook, J. J.; Holahan, M. A.; Stranieri-Michener, M.; Leonard, Y. M.; Lynch, J. J. Jr.; McMasters, D. R.; Yan, Y. 9-Hydroxyazafluorenes and their use in thrombin inhibitors. *J. Med. Chem.* **2005**, *48*, 2282−2293.
(30) Baum, B.; Muley, L.; Heine, A.; Smolinski, M.; Hangauer, D.; Klebe, G. Think twice: understanding the high potency of bis(phenyl)methane inhibitors of thrombin. *J. Mol. Biol.* **2009**, *391*, 552−564.
(31) Kadono, S.; Sakamoto, A.; Kikuchi, Y.; Oh-eda, M.; Yabuta, N.; Yoshihashi, K.; Kitazawa, T.; Suzuki, T.; Koga, T.; Hattori, K.; Shiraishi, T.; Haramura, M.; Kodama, H.; Ono, Y.; Esaki, T.; Sato, H.; Watanabe, Y.; Itoh, S.; Ohta, M.; Kozono, T. Structure-based design of P3 moieties in the peptide mimetic factor VIIa inhibitor. *Biochem. Biophys. Res. Commun.* **2005**, *327*, 589−596.
(32) Dullweber, F.; Stubbs, M. T.; Musil, D.; Stürzebecher, J.; Klebe, G. Factorising ligand affinity: a combined thermodynamic and crystallographic study of trypsin and thrombin inhibition. *J. Mol. Biol.* **2001**, *313*, 593−614.
(33) Hanessian, S.; Yang, G.; Rondeau, J. M.; Neumann, U.; Betschart, C.; Tintelnot-Blomley, M. Structure-based design and synthesis of macroheterocyclic peptidomimetic inhibitors of the aspartic protease beta-site amyloid precursor protein cleaving enzyme (BACE). *J. Med. Chem.* **2006**, *49*, 4544−4567.

(34) Boger, D. L.; Yohannes, D. Total synthesis of deoxybouvardin and RA-VII: macrocyclization via an intramolecular Ullmann reaction. *J. Am. Chem. Soc.* **1991**, *113*, 1427−1429.
(35) Boger, D. L.; Yohannes, D.; Zhou, J.; Patane, M. A. Total synthesis of cycloisodityrosine, RA-VII, deoxybouvardin, and N29-desmethyl-RA-VII: identification of the pharmacophore and reversal of the subunit functional roles. *J. Am. Chem. Soc.* **1993**, *115*, 3420−3430.
(36) Boger, D. L.; Zhou, J. *N*-Desmethyl derivatives of deoxybouvardin and RA-VII: synthesis and evaluation. *J. Am. Chem. Soc.* **1995**, *117*, 7364−7378.
(37) Marder, V. J.; Jahan, R.; Gruber, T.; Goyal, A.; Arora, V. Thrombolysis with plasmin: implications for stroke treatment. *Stroke* **2010**, *41*, S45−S49.
(38) Ramírez-López, P.; La Torre, M. C.; Montenegro, H. E.; Asenjo, M.; Sierra, M. A. A straightforward synthesis of tetrameric estrone-based macrocycles. *Org. Lett.* **2008**, *10*, 3555−3558.
(39) *SYBYL*, version 8.0; Tripos International: St. Louis, MO.
(40) Plewczynski, D.; Lazniewski, M.; Augustyniak, R.; Ginalski, K. Can we trust docking results? Evaluation of seven commonly used programs on PDBbind database. *J. Comput. Chem.* **2011**, *32*, 742−755.
(41) *MOE*, version 2010; Chemical Computing Group: Montreal, Canada.
(42) Labute, P. LowModeMD—implicit low-mode velocity filtering applied to conformational search of macrocycles and protein loops. *J. Chem. Inf. Model.* **2010**, *50*, 792−800.
(43) *LeadIT*, version 2.0.1; BioSolveIT GmbH: Sankt Augustin, Germany.